Accurate 2D MoM Technique for Arbitrary Dielectric, Magnetic and Conducting Media Applied to Shielding Problems

Dieter Dobbelaere, Hendrik Rogier, Daniel De Zutter

Electromagnetics Group, Department of Information Technology, Ghent University
Sint-Pietersnieuwstraat 41, Ghent, Belgium

***Abstract*—Calculating interaction integrals in a Method of Moments technique is highly challenging in a conductive medium. The specific form of its wave number leads to a strongly oscillating and exponentially damped Green's function, making standard numerical evaluation schemes inapt to accurately evaluate the interaction integrals. In this paper, we present an accurate 2D Method of Moments technique for arbitrary dielectric, magnetic and conducting media and apply the method to solve shielding problems.**

I. Introduction

Numerical frequency domain techniques based on the Method of Moments (MoM) require an evaluation of interaction integrals with a Green's function and its derivatives as integral kernels. In this paper, we study a two-dimensional geometry and a coupled TE/TM problem where the sources and fields have an $e^{j(\omega t-\beta z)}$ dependence along the longitudinal z coordinate. The interaction integrals arising in the MoM system matrix need to be accurately evaluated, taking into account the difficulties associated with the singular behavior of their integrands.

In low-loss dielectrics, both singularity extraction [1], [2], [3] and cancellation [4], [5], [6] has been used to successfully deal with the singularities of the Green's function and its derivatives. In conductive media, additional difficulties originate from the rapid decay of the amplitude of the Green's function (see [7] for the three-dimensional case), making standard techniques in dielectric media inapt to accurately evaluate the interaction integrals.

A dedicated method based on singularity extraction for the evaluation of 2D interaction integrals in conductive media, is presented here, efficiently dealing with both the singular behavior of the integrands and the rapid decay of the Green's function. The method is applied to shielding problems, showing its correctness and accuracy.

II. Geometry and Boundary Integral Equations

The considered geometry is invariant in the z direction and consists of linear piecewise homogeneous isotropic material regions Ω_i with complex permittivity ϵ_i and permeability μ_i (Fig. 1). If all sources and fields have a common $e^{j(\omega t-\beta z)}$ dependence ($\beta \in \mathbb{C}$), the representation formulae (1)-(2) (see next page) at boundary point $\boldsymbol{\rho}_b \in \partial\Omega_i$ hold if medium Ω_i contains no sources (with $\gamma_i^2 = \omega^2\epsilon_i\mu_i - \beta^2$) [8]. Similar expressions are found for the longitudinal and transversal tangential magnetic field, $H_z(\boldsymbol{\rho}_b)$ and $H_t(\boldsymbol{\rho}_b)$, respectively, via well-known duality substitutions. The Green's function of medium i is the fundamental solution of the two-dimensional Helmholtz operator that satisfies the Sommerfeld radiation condition, i.e. $G_i(\boldsymbol{\rho}|\boldsymbol{\rho}') = \frac{j}{4}H_0^{(2)}(\gamma_i|\boldsymbol{\rho}-\boldsymbol{\rho}'|)$, with the branch cuts chosen such that $-\pi < \arg\gamma_i(\beta) \leq 0$. After imposing tangential field continuity at the boundaries, a linear system arises between the sources and the longitudinal and transverse tangential fields at the boundaries.

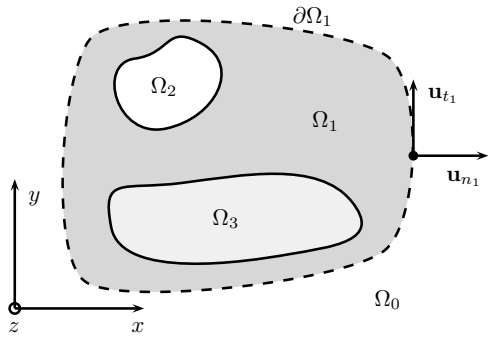

Fig. 1. Geometry consisting of piecewise homogeneous isotropic material regions

III. Interaction Integrals

After a discretisation of the material boundaries $\partial\Omega_i$ into a union (notation Γ_i) of straight segments S_j, the transverse tangential and longitudinal boundary field components are expanded into pulse functions $p_j(\boldsymbol{\rho})$ and triangular functions $t_j(\boldsymbol{\rho})$, respectively:

$$p_j(\boldsymbol{\rho}) = \frac{1}{l_j} \qquad \boldsymbol{\rho} \in S_j, \tag{1}$$

$$t_j(\boldsymbol{\rho}) = \begin{cases} 1 - |\boldsymbol{\rho} - \boldsymbol{\rho}_{j+1}|\ l_j^{-1} & \boldsymbol{\rho} \in S_j \\ 1 - |\boldsymbol{\rho} - \boldsymbol{\rho}_{j+1}|\ l_{j+1}^{-1} & \boldsymbol{\rho} \in S_{j+1}, \end{cases} \tag{2}$$

where segment S_j has length l_j and is bounded by the points $\boldsymbol{\rho}_j$ and $\boldsymbol{\rho}_{j+1}$. Field components expanded into pulse functions are tested with triangular functions, and vice versa, yielding

a Petrov-Galerkin scheme with the following prototype MoM interaction integrals:

$$\mathsf{I}_{jk}^{\mathsf{pp}} = \int_{\Gamma_i} p_j(\boldsymbol{\rho})\ dc \int_{\Gamma_i} G_i(\boldsymbol{\rho}|\boldsymbol{\rho}')\ p_k(\boldsymbol{\rho}')\ dc', \tag{3}$$

$$\mathsf{I}_{jk}^{\mathsf{pt}} = \int_{\Gamma_i} p_j(\boldsymbol{\rho})\ dc \int_{\Gamma_i} \frac{\partial G_i(\boldsymbol{\rho}|\boldsymbol{\rho}')}{\partial n'}\ t_k(\boldsymbol{\rho}')\ dc', \tag{4}$$

$$\mathsf{I}_{jk}^{\mathsf{tt}} = \int_{\Gamma_i} t_j(\boldsymbol{\rho})\ dc \int_{\Gamma_i} \frac{\partial^2 G_i(\boldsymbol{\rho}|\boldsymbol{\rho}')}{\partial n \partial n'}\ t_k(\boldsymbol{\rho}')\ dc'. \tag{5}$$

This can be seen by inspecting (1)-(2) and transferring the tangential derivative of the Green's function to the test function using Stokes' theorem. The inner integral of (5) should be interpreted in a finite part sense.

IV. Difficulties in Conductive Media

In a conductive medium with electric conductivity σ, permittivity $\epsilon = \epsilon_r\epsilon_0 + \frac{\sigma}{j\omega}$ and permeability $\mu = \mu_r\mu_0$, one can easily prove that for excitations with $\beta \leq \omega\sqrt{\epsilon_0\mu_0}$ (which propagate in the background medium) and for operating frequencies $\omega = 2\pi f \ll \frac{\sigma}{\epsilon_r\epsilon_0}$, the transversal wave number is given by:

$$\gamma \approx \frac{1-j}{\delta}, \tag{6}$$

with the skin depth of the conductor equal to $\delta = (\pi f \mu \sigma)^{-1/2}$. The Green's function and its normal derivatives in (3)-(5) can be written as a linear combination of Hankel functions of the second kind of order $\nu \in \{0, 1, 2\}$. For large arguments, these functions behave as [9]

$$H_\nu^{(2)}(\gamma r) \approx \sqrt{\frac{2}{\pi\gamma r}} e^{-j\gamma r + j\frac{\pi}{4}(2\nu+1)} \qquad (|\arg \gamma r| < \pi). \tag{7}$$

As the skin depth is much smaller than the free space wavelength $\lambda_0 = (f\sqrt{\epsilon_0\mu_0})^{-1}$ for the considered frequencies, the interaction integral kernels in a conductive medium are highly oscillatory and exponentially damped over a segment.

Numerical evaluation schemes for the interaction integrals in low-loss dielectrics, such as a Gauss-Legendre (GL) quadrature rule over both test and source segment with singularity extraction, fail to correctly evaluate (3)-(5) in a conductive medium. As an example, let us consider a segment S_j that lies on the boundary between the conductive medium (with σ =5.8e7 S/m, $\epsilon_r = 1$ and $\mu_r = 1$) and a free space medium. As a rule of thumb, it is sufficient to choose the segment length equal to a fraction of the free space wavelength, say $l_j = \lambda_0/10$, in order to capture the field variations. Figure 2 shows the relative error made when calculating the selfpatch term $\mathsf{I}_{jj}^{\mathsf{pp}}$ with an $N_q \times N_q$ GL quadrature rule with singularity extraction. The exact value of the integral was calculated with an adaptive quadrature rule of Maple®. Even for the highest quadrature orders, the evaluated integral differs several orders of magnitude from its exact value.

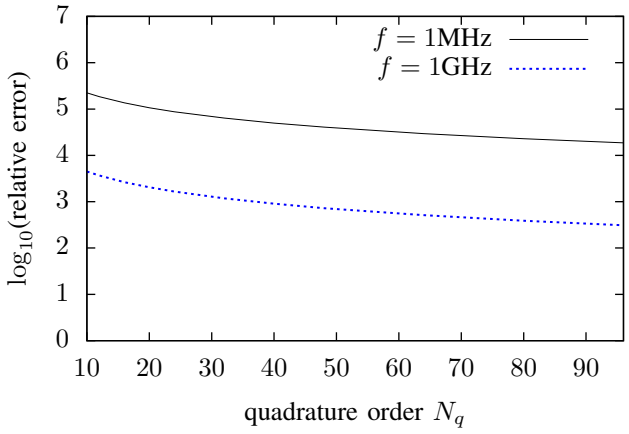

Fig. 2. Error, relative w.r.t. the exact value, on the selfpatch term $\mathsf{I}_{jj}^{\mathsf{pp}}$ using an $N_q \times N_q$ GL quadrature rule with singularity extraction.

V. Proposed Method

In order to accurately evaluate the interaction integrals (3)-(5), the integration domain is confined to a set in which the source and observation points are sufficiently close to each other. Given a threshold parameter Δ_{cut}, we define the cut-off distance r_{cut} in the conductive medium as the distance above which the amplitude of the Green's function is smaller than Δ_{cut}. It can be shown that this leads to expression (8) (for sufficiently small Δ_{cut}, such that (7) holds), with $\mathcal{W}$ the principal branch of the Lambert W function [10].

$$r_{\mathsf{cut}} = \frac{\delta}{2}\mathcal{W}\left(\frac{1}{4\pi\sqrt{2}\Delta_{\mathsf{cut}}^2}\right). \tag{8}$$

$$E_z(\boldsymbol{\rho}_b) = \lim_{\boldsymbol{\rho}\to\boldsymbol{\rho}_b} \oint_{\partial\Omega_i} \left[E_z(\boldsymbol{\rho}')\frac{\partial G_i(\boldsymbol{\rho}|\boldsymbol{\rho}')}{\partial n'} - \left(\frac{j\gamma_i^2}{\omega\epsilon_i}H_t(\boldsymbol{\rho}') - \frac{\beta}{\omega\epsilon_i}\frac{\partial H_z(\boldsymbol{\rho}')}{\partial t'}\right) G_i(\boldsymbol{\rho}|\boldsymbol{\rho}')\right] dc', \tag{1}$$

$$\begin{aligned} E_t(\boldsymbol{\rho}_b) = \lim_{\boldsymbol{\rho}\to\boldsymbol{\rho}_b} \oint_{\partial\Omega_i} \Bigg[& \frac{j\omega\mu_i}{\gamma_i^2}H_z(\boldsymbol{\rho}')\frac{\partial^2 G_i(\boldsymbol{\rho}|\boldsymbol{\rho}')}{\partial n \partial n'} + \frac{j\omega\mu_i}{\gamma_i^2}\left(\frac{j\gamma_i^2}{\omega\mu_i}E_t(\boldsymbol{\rho}') - \frac{\beta}{\omega\mu_i}\frac{\partial E_z(\boldsymbol{\rho}')}{\partial t'}\right)\frac{\partial G_i(\boldsymbol{\rho}|\boldsymbol{\rho}')}{\partial n} \\ & - \frac{j\beta}{\gamma_i^2}E_z(\boldsymbol{\rho}')\frac{\partial^2 G_i(\boldsymbol{\rho}|\boldsymbol{\rho}')}{\partial t \partial n'} + \frac{j\beta}{\gamma_i^2}\left(\frac{j\gamma_i^2}{\omega\epsilon_i}H_t(\boldsymbol{\rho}') - \frac{\beta}{\omega\epsilon_i}\frac{\partial H_z(\boldsymbol{\rho}')}{\partial t'}\right)\frac{\partial G_i(\boldsymbol{\rho}|\boldsymbol{\rho}')}{\partial t}\Bigg] dc'. \end{aligned} \tag{2}$$

The integrals are now approximated by

$$\mathsf{I}^{\mathsf{pp}}_{jk} \approx \int_{\Gamma_i} p_j \; dc \int_{\Gamma_i} G_i \mathbb{H}(r_{\mathsf{cut}} - |\boldsymbol{\rho} - \boldsymbol{\rho}'|) \; p_k \; dc', \tag{9}$$

$$\mathsf{I}^{\mathsf{pt}}_{jk} \approx \int_{\Gamma_i} p_j \; dc \int_{\Gamma_i} \frac{\partial G_i}{\partial n'} \mathbb{H}(r_{\mathsf{cut}} - |\boldsymbol{\rho} - \boldsymbol{\rho}'|) \; t_k \; dc', \tag{10}$$

$$\mathsf{I}^{\mathsf{tt}}_{jk} \approx \int_{\Gamma_i} t_j \; dc \int_{\Gamma_i} \frac{\partial^2 G_i}{\partial n \partial n'} \mathbb{H}(r_{\mathsf{cut}} - |\boldsymbol{\rho} - \boldsymbol{\rho}'|) \; t_k \; dc', \tag{11}$$

with $\mathbb{H}$ the Heaviside step function. Explicit bounds on the approximation errors can be obtained as a function of Δ_{cut}. For the singular or nearly-singular integrands, a singularity extraction technique is employed, and explicit forms of the extracted singular parts with limited support can be found.

VI. Numerical Examples

Consider a conductive square shielding tube immersed in free space (Fig. 3). Suppose the dimensions of the tube are $a = 40$ cm and $t = 0.5$ mm and the conductive material is copper ($\sigma = 5.8e7$ S/m and $\mu_r = 1$). In this example, we will study the low-frequency shielding properties of the tube for different kinds of external excitations, and look at the effect of a magnetic coating covering the outside of the tube (Fig. 4). In the sequel, we always use a fixed thickness of the coating layers $t_d = t_m = 0.1$ mm, but consider the influence of the number of magnetic layers.

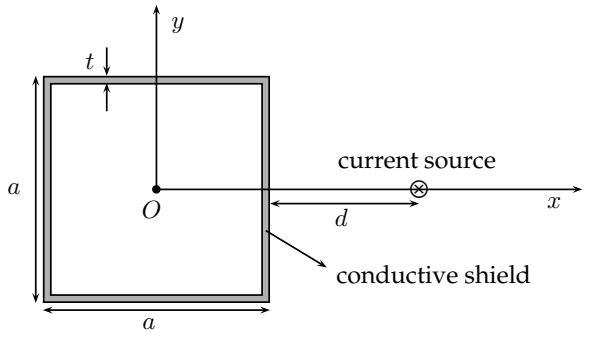

Fig. 3. Conductive square shielding tube with exterior dipole source.

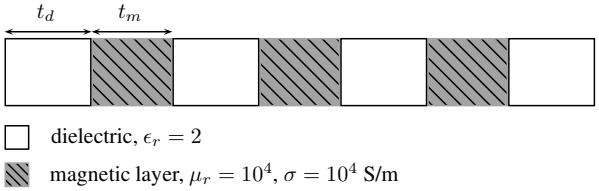

Fig. 4. Coating consisting of three magnetic layers with thickness t_m, sandwiched between dielectric layers with thickness t_d.

Let us define the shielding factor as the ratio between the energy density of the fields at the center of the tube, with and without shield, i.e.

$$S = 10 \log_{10} \left[\frac{\epsilon_0 |\mathbf{E}_0|^2 + \mu_0 |\mathbf{H}_0|^2}{\epsilon_0 |\mathbf{E}|^2 + \mu_0 |\mathbf{H}|^2} \right]_{\text{at } O} \quad \text{(dB)}. \tag{12}$$

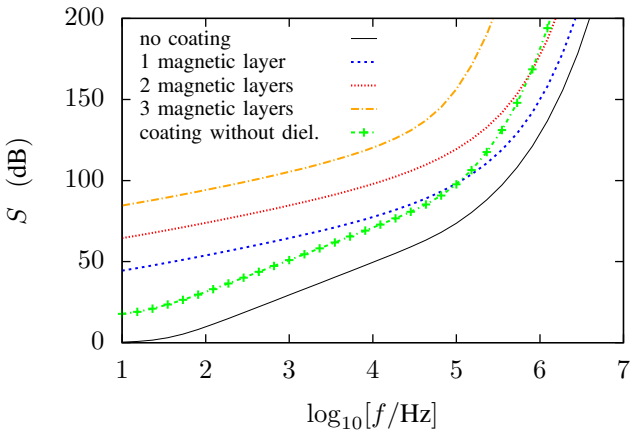

Fig. 5. Shielding factor S for an electric current source at $d = 1$ m, for a number of coatings.

A. Electric current excitation

An electric current excitation $\mathbf{j} = I\delta(x - \frac{a}{2} - d, y)\mathbf{u}_z$ leads to a low impedance near field, as

$$Z_s = \left| \frac{\mathbf{E}}{\mathbf{H}} \right| = Z_0 \left| \frac{H_0^{(2)}(k_0 r)}{H_1^{(2)}(k_0 r)} \right| \sim -Z_0 k_0 r \ln(k_0 r), \tag{13}$$

for $k_0 r \to 0$, such that most of the electromagnetic energy is stored in the magnetic field. This source can be a good model for an external source which generates a dominant magnetic field, such as power transformers or overhead power lines.

Fig. 5 shows the shielding factor for such an electric current source at $d = 1$ m. As expected, a conductive tube without coating is a very poor shield against quasi-static magnetic fields. The shielding properties greatly enhance when a coating is added at the outside of the conductor, with its dimensions and material parameters as defined above. The highest increase in shielding factor is found between no layer and one layer. The addition of each extra magnetic layer adds about 20 dB extra shielding at low frequencies. The curve of the coating without dielectrics in Fig. 5 shows the effect if the dielectric spacers between the magnetic layers are omitted, now considering a magnetic layer with a thickness $3t_m$. At low frequencies, this coating performs worse than a coating with a magnetic layer of thickness t_m *with* dielectrics. This can be explained by the high contrast in wave impedance between the magnetic and dielectric layers, which causes additional reflection. At high frequencies, it performs better than a one or two layer coating with dielectrics, as now the exponential decay inside the magnetic layer will start to dominate.

B. Magnetic current excitation

A magnetic current excitation $\mathbf{m} = M\delta(x - \frac{a}{2} - d, y)\mathbf{u}_z$ has a high impedance near field, and it is a good model for an

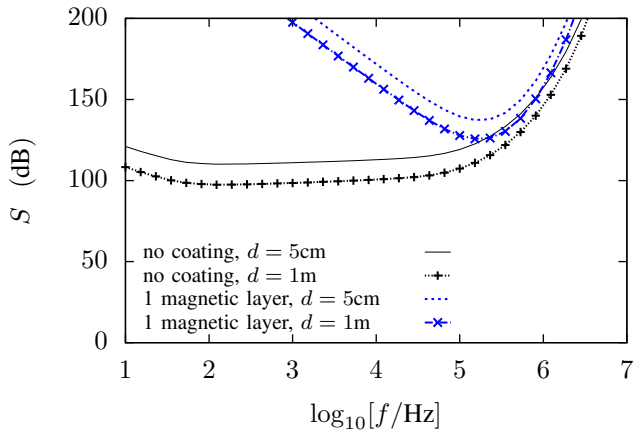

Fig. 6. Shielding factor S for a magnetic current source, located at two distances.

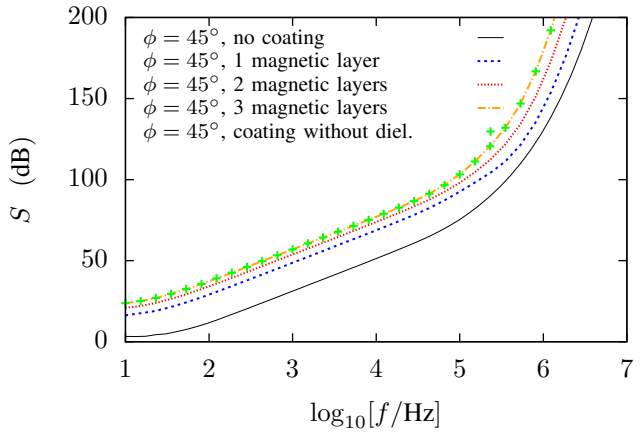

Fig. 7. Shielding factor S for an obliquely incident plane wave excitation.

external noise source which generates a dominant electric field, for example the near field of a dipole antenna. It can be seen from Fig. 6 that the conductive tube without coating already shows a very good shielding performance for low frequency electric fields, and this effect is only enhanced by adding a coating with one magnetic layer. For high frequencies, the absorption loss inside the conductive layers dominates, whereas for low frequencies, the reflection loss at the outer interface becomes dominant. For an infinite plane shield, this reflection loss increases when the distance between shield and excitation decreases. In our example, we found that $S \sim 1/(a/2 + d)$ at low frequencies, i.e. the shielding factor is inversely proportional to the distance between the tube's centre and the excitation.

C. Plane wave excitation

Figure 7 shows the shielding factor for an obliquely incident plane wave with wave vector $\mathbf{k} = k_0(-\cos\phi, 0, \sin\phi)$, linearly polarized with the electric field along the y direction. For high frequencies, the absorption loss inside the conductive layers leads to a good shielding performance. The conductive shield without coating yields a low shielding factor for low frequencies, but it can be increased by adding a coating. It can also be seen that the dielectric layers between the coating have little effect on the overall shielding factor, as opposed to the case with an electric current.

REFERENCES

[1] D. Wilton, S. Rao, A. Glisson, D. Schaubert, O. Al-Bundak, and C. Butler, "Potential integrals for uniform and linear source distributions on polygonal and polyhedral domains," *Antennas and Propagation, IEEE Transactions on*, vol. 32, no. 3, pp. 276 – 281, Mar. 1984.

[2] P. Yla-Oijala and M. Taskinen, "Calculation of CFIE impedance matrix elements with RWG and n $\times$ RWG functions," *Antennas and Propagation, IEEE Transactions on*, vol. 51, no. 8, pp. 1837 – 1846, Aug. 2003.

[3] R. Graglia, "On the numerical integration of the linear shape functions times the 3-D Green's function or its gradient on a plane triangle," *Antennas and Propagation, IEEE Transactions on*, vol. 41, no. 10, pp. 1448 –1455, Oct. 1993.

[4] M. Khayat and D. Wilton, "Numerical evaluation of singular and near-singular potential integrals," *Antennas and Propagation, IEEE Transactions on*, vol. 53, no. 10, pp. 3180 – 3190, Oct. 2005.

[5] R. Graglia and G. Lombardi, "Machine precision evaluation of singular and nearly singular potential integrals by use of Gauss quadrature formulas for rational functions," *Antennas and Propagation, IEEE Transactions on*, vol. 56, no. 4, pp. 981 –998, Apr. 2008.

[6] A. Polimeridis and J. Mosig, "Evaluation of weakly singular integrals via generalized cartesian product rules based on the double exponential formula," *Antennas and Propagation, IEEE Transactions on*, vol. 58, no. 6, pp. 1980 –1988, Jun. 2010.

[7] J. Peeters, I. Bogaert, and D. De Zutter, "Calculation of MoM interaction integrals in highly conductive media," *Antennas and Propagation, IEEE Transactions on*, vol. 60, no. 2, pp. 930 –940, Feb. 2012.

[8] F. Olyslager, D. De Zutter, and K. Blomme, "Rigorous analysis of the propagation characteristics of general lossless and lossy multiconductor transmission lines in multilayered media," *Microwave Theory and Techniques, IEEE Transactions on*, vol. 41, no. 1, pp. 79 –88, Jan. 1993.

[9] G. Watson, *A Treatise on the Theory of Bessel Functions*, ser. Cambridge Mathematical Library. Cambridge University Press, 1995.

[10] F. Olver, D. Lozier, R. Boisvert, and C. Clark, *NIST Handbook of Mathematical Functions*. Cambridge University Press, 2010.